JOURNAL OF VIROLOGY, Sept. 1998, p. 7245–7254 Vol. 72, No. 9
0022-538X/98/$04.00+0

The Disulfide-Bonded Structure of Feline Herpesvirus Glycoprotein I

J. D. F. MIJNES, B. C. H. LUTTERS, A. C. VLOT, M. C. HORZINEK, P. J. M. ROTTIER, AND R. J. DE GROOT*

Virology Unit, Department of Infectious Diseases and Immunology, Veterinary Faculty, Utrecht University, 3584 CL Utrecht, The Netherlands

Received 10 April 1998/Accepted 11 June 1998

Alphaherpesvirus glycoproteins E and I (gE and gI, respectively) assemble into a hetero-oligomeric complex which promotes cell-to-cell transmission, a determining factor of virulence. Focusing on gI of feline herpesvirus (FHV), we examined the role of disulfide bonds during its biosynthesis, its interaction with gE, and gE-gI-mediated spread of the infection in vitro. The protein's disulfide linkage pattern was determined by single and pairwise substitutions for the four conserved cysteine residues in the ectodomain. The resulting mutants were coexpressed with gE in the vaccinia virus-based vTF7-3 system, and the formation and endoplasmic reticulum (ER)-to-Golgi transport of the hetero-oligomeric complex were monitored. The results were corroborated biochemically by performing an endoproteinase Lys-C digestion of a [^{35}S]Cys-labeled secretory recombinant form of gI followed by tricine-sodium dodecyl sulfate-polyacrylamide gel electrophoresis analysis of the peptides under reducing and nonreducing conditions. We found that (i) gI derivatives lacking Cys^{79} (C_1) and/or Cys^{223} (C_4) still assemble with gE into transport-competent complexes, (ii) mutant proteins lacking Cys^{91} (C_2) and/or Cys^{102} (C_3) bind to gE but are retained in the ER, (iii) radiolabeled endoproteinase Lys-C-generated peptide species containing C_1 and C_4 are linked through disulfide bonds, and (iv) peptides containing both C_2 and C_3 are not disulfide linked to any other peptide. From these findings emerges a model in which C_1 and C_4 as well as C_2 and C_3 form intramolecular disulfide bridges. Since the cysteines in the ectodomain have been conserved during alphaherpesvirus divergence, we postulate that the model applies for all gI proteins. Analysis of an FHV recombinant with a $C_1 \rightarrow S$ substitution confirmed that the C_1-C_4 disulfide bond is not essential for the formation of a transport-competent gE-gI complex. The mutation affected the posttranslational modification of gI and caused a slight cold-sensitivity defect in the assembly or the intracellular transport of the gE-gI complex but did not affect plaque size. Thus, C_1 and the C_1-C_4 bond are not essential for gE-gI-mediated cell-to-cell spread, at least not in vitro.

The alphaherpesvirus glycoproteins E and I (gE and gI, respectively) form a hetero-oligomeric complex which is found in the viral envelope and at the surface of the infected cell (23, 38, 53, 54, 58, 61). Although dispensable for replication in cultured cells, the genes for gE and gI are conserved in all alphaherpesviruses studied to date (4, 11, 29, 36, 41, 43, 48, 54, 55). Infection experiments in both natural and experimental hosts indicate that the gE-gI complex is an important virulence factor: viruses deficient for gE and/or gI produce milder clinical signs, cause smaller primary lesions, and exhibit a lower degree of neuronal spread than the wild-type virus (8, 11, 12, 18, 27, 28, 40, 44, 48, 50, 53, 55).

Recently, Knapp and Enquist reported that the virulence of a pseudorabies virus (PRV) mutant deficient for gE and gI could be restored by complementation with gE and gI of bovine herpesvirus (26). This result suggests that gE-gI complexes of different alphaherpesviruses are functionally equivalent. However, the function of the gE-gI hetero-oligomer is not exactly known. For some herpesviruses, the gE-gI complex functions as a receptor for the Fc domain of immunoglobulin G and, consequently, may play a role in the evasion of humoral immunity (5, 6, 13, 14, 19, 20, 24, 30, 51). Most evidence, however, indicates that the gE-gI complex is primarily involved in cell-to-cell transmission, possibly by promoting cell fusion or virus release (4, 10–12, 60). Cell-to-cell spread differs in several respects from virus entry and apparently entails the transfer of the virus across cell junctions in a manner resistant to neutralizing antibodies (4, 11, 60). In vitro, virus mutants lacking gE and/or gI characteristically display a small-plaque phenotype (4, 11, 36, 37, 41, 48, 54, 60).

The biosynthesis of the gE-gI complex has been studied in detail for several alphaherpesviruses, and from this work the following picture emerges. The proteins are synthesized in the endoplasmic reticulum (ER) as N-glycosylated class I membrane proteins which readily assemble into noncovalently linked hetero-oligomeric complexes, most likely heterodimers (23, 25, 38, 53, 54, 58, 61). These are transported along the secretory pathway, concomitantly acquiring extensive posttranslational modifications: elaborate processing of the N-linked oligosaccharides, addition of O-linked oligosaccharides, and sulfatation, as well as phosphorylation (15, 16, 23, 30, 38, 43, 53, 54, 57, 58).

gE and gI both possess large cytoplasmic domains. In varicella-zoster virus, these domains contain signals that mediate cycling of the complex between the plasma membrane, the endosomes, and the trans-Golgi network (1, 42, 59). The cytoplasmic tails of gE and gI are dispensable, however, for complex formation (25, 37, 49). In the case of feline herpesvirus (FHV), a C-terminally truncated gI derivative of 166 residues (corresponding to the N-terminal half of the ectodomain) still assembles into a transport-competent complex with gE. An even shorter derivative, comprising the 93 N-terminal residues, can still bind to gE to yield a stable hetero-oligomer, but this complex is transport incompetent (37). These observations suggest that the N-terminal region of gI is involved in the

* Corresponding author. Mailing address: Virology Unit, Department of Infectious Diseases and Immunology, Faculty of Veterinary Medicine, Utrecht University, Yalelaan 1, 3584 CL Utrecht, The Netherlands. Phone: 31-30-2533337. Fax: 31-30-2536723. E-mail: R.Groot@vet.uu.nl.

TABLE 1. Oligonucleotide primers used in these studies

Primer	Nucleotide sequence (5′ to 3′)	Gene	Positions[a]	Polarity
569	TCTTCTTCCTATAAAATCGTTCAAGTA	gI	229–255	+
570	TTTATAGGAAGAAGAGTGATGGTTGTA	gI	217–243	−
581	TCATCATCTCCACGTGTACGCAATAAT	gI	265–291	+
582	ACGTGGAGATGATGAATATTCTATTAC	gI	253–279	−
603	CGGTCCTCTCTCCACAAGACCTCTATG	gI	298–324	+
604	GTGGAGAGAGGACCGGAAAGCATTATT	gI	286–312	−
630	TTAACGTCTCGCCCACGTTAT	gE	1168–1188	−
633	TTAGTGGTGGTGGTGGTGGTGCTTTCTGTCTGGTGTCCA	gI	850–867	−

[a] Numerical positions on the genome of FHV B927 as counted from the initiation codon of gE or gI.

interaction with gE, a notion supported by the observation that for varicella-zoster virus, mutations in the very N terminus of gI abolish complex formation (25).

Apparently, gE-gI function is primarily effectuated by the ectodomains. Deletion of the cytoplasmic tail of FHV gI only marginally affects plaque size (37). Furthermore, the cytoplasmic tail of PRV gE is dispensable for gE-gI-mediated neuronal spread. Upon retinal infection of rats, mutant viruses expressing truncated gE retained the ability to spread to all retinorecipient regions of the brain (49).

The ectodomains of gE and gI contain cysteine residues which are strictly conserved and are likely to form intramolecular disulfide bridges that stabilize the protein conformation. The cysteine map of gI is remarkably similar to those of two other short unique region-encoded alphaherpesvirus glycoproteins, gG and gD, in that they share a characteristic motif, $C\text{-}X_{11}\text{-}C\text{-}X_{8-10}\text{-}C$. This observation has led McGeoch (34) to postulate that gG, gD, and gI are evolutionary related and have arisen through gene duplication. The hypothesis predicts that gG, gD, and gI have similar disulfide-bonded structures (32). Another corollary of the hypothesis is that the formation of the conserved disulfide bonds must be important for the folding and/or function of these proteins: if gG, gD, and gI are related, they are separated by a large evolutionary distance, and the cysteine residues would not have been conserved unless their loss had entailed a decrease in viral fitness. The disulfide-bonded structure has been solved for the gD of herpes simplex virus (HSV) types 1 and 2 (32). Of the cysteines in the motif, the two C-terminal-most residues form a disulfide bond, yielding a small 8-residue loop; the N-terminal-most cysteine pairs with a fourth residue downstream of the motif.

Here, we have studied the disulfide bridges of a gI protein. We have probed the disulfide-bonded structure of FHV gI both by site-directed mutagenesis of cysteine residues and by biochemical analysis of the purified protein. The effects of Cys→Ser substitutions on gE-gI complex formation and intracellular transport and on gE-gI-mediated cell-to-cell spread are discussed.

MATERIALS AND METHODS

Cells, viruses, antisera, and plasmids. Cells were maintained in Dulbecco's modified Eagle's medium (DMEM; Gibco BRL, Life Technologies, Inc.) supplemented with 10% fetal calf serum and 100 IU of penicillin and 100 μg of streptomycin per ml (DMEM–10% FCS). FHV strain B927 (22) was obtained from D. A. Harbour and propagated in Crandell feline kidney (CRFK) cells (American Type Culture Collection) (9). Recombinant vaccinia virus vTF7-3, expressing the bacteriophage T7 RNA polymerase (21), was obtained from B. Moss and propagated in RK-13 cells. Transient expression experiments were performed in OST7-1 cells (17). The monospecific rabbit antisera against FHV gE (Ra-αgE) and gI (Ra-αgI), the cat antiserum against FHV (Cat-αFHV), and the plasmids pBS-gE, pBS-gI, pBS-gIΔM, and pUS1 have been described previously (37, 38).

Recombinant DNA techniques. Recombinant DNA techniques were performed according to the procedures of Sambrook et al. (46) and Ausubel et al. (3). Sequence analysis was performed with a T7 sequencing kit (Pharmacia Biotech). PCR was performed as described elsewhere (45), using the thermostable DNA polymerase of *Thermus aquaticus* (*Taq* polymerase; Gibco BRL, Life Technologies, Inc.) in accordance with the instructions of the manufacturer.

Mutagenesis of pBS-gIΔM. pBS-gIΔM was constructed by cutting pBS-gI with *Mlu*I, which cuts at nucleotide (nt) 497, and with *Xba*I, which cuts at a site downstream of the gI gene within the polylinker region of pBS-SK$^-$. The 3′ recessive ends were filled in, using the large fragment of DNA polymerase I (Gibco BRL, Life Technologies, Inc.), and ligated. To replace Cys^{79} (C_1) with Ser, two overlapping oligonucleotide primers of opposite polarity, no. 569 and no. 570 (Table 1), were designed, both of which directed a G^{236}→C substitution. The 5′ and 3′ halves of the gIΔM gene were PCR amplified with oligonucleotide 570 plus the M13 universal primer and with oligonucleotide 569 plus the M13 reverse primer, respectively. The PCR products were purified from low-melting-point agarose; 5 ng of each was mixed in a 50-μl volume of PCR buffer and denatured by incubation for 5 min at 95°C. After reannealing, heterologous DNA hybrids were elongated with *Taq* polymerase and a PCR was performed with the M13 universal and reverse primers to amplify the complete $gI\Delta M\Delta C_1$ gene. The resulting PCR product was digested with *Pml*I, which cuts at nt 277, and with *Hin*dIII, which cuts at a site upstream of the gIΔM gene within the polylinker region. The 292-bp *Pml*I-*Hin*dIII fragment was gel purified and exchanged for the corresponding sequences in pBS-gIΔM, yielding $pBS\text{-}gI\Delta M\Delta C_1$. Mutagenesis of Cys^{91} (C_2) and Cys^{102} (C_3) was performed accordingly, with primer pairs 582-581 and 604-603, respectively. To obtain $pBS\text{-}gI\Delta M\Delta C_2$ and $pBS\text{-}gI\Delta M\Delta C_3$, the PCR products obtained were cut with *Pml*I and *Hin*dIII or *Not*I, respectively; the *Not*I site is located within the polylinker region downstream of the gIΔM gene. The 292-bp *Pml*I-*Hin*dIII and 229-bp *Pml*I-*Not*I fragments were purified from the gel and exchanged with the corresponding sequences in pBS-gIΔM, yielding $pBS\text{-}gI\Delta M\Delta C_2$ and $pBS\text{-}gI\Delta M\Delta C_3$, respectively. $pBS\text{-}gI\Delta M\Delta C_{23}$ was constructed by inserting the *Pml*I-*Hin*dIII fragment of $pBS\text{-}gI\Delta M\Delta C_2$ into *Pml*I- and *Hin*dIII-digested $pBS\text{-}gI\Delta M\Delta C_3$. To construct $pBS\text{-}gI\Delta MC_0$, C_1 in $pBS\text{-}gI\Delta M\Delta C_{23}$ was replaced by Ser via PCR mutagenesis as described above. Sequence analysis of the relevant regions of each construct confirmed that no inadvertent nucleotide changes had occurred during PCR amplification and cloning.

Construction of plasmids pBS-sgE and pBS-sgI. To construct pBS-sgE, a PCR was performed with the M13 universal primer and primer 630 (Table 1), using plasmid pBS-gE (38) as a template. The PCR product was blunt ended with the large fragment of DNA polymerase I and digested with *Sna*BI. The resulting 204-bp fragment (nt 985 to 1188) was gel purified and inserted into the 4-kb *Sna*BI-*Sal*I (blunt) fragment of pBS-gE, yielding pBS-sgE. In pBS-sgE, nt 1186 through 1599 of the gE gene were deleted and a termination codon was created downstream of the codon for Arg^{395}.

pBS-sgI was made as follows. pBS-gI (38) served as a template for PCR with the M13 universal primer and primer 633 (Table 1). The PCR product was blunt ended and subsequently cut with *Mlu*I. Thus, a 393-bp fragment was generated, which was gel purified and ligated to the 2.6-kb *Eco*RI (blunt)-*Mlu*I fragment of pBS-gI. As a result of the cloning procedure, nt 869 through 1155 of the gI gene were deleted and a termination codon was created downstream of the codon for Lys^{289}. Sequence analysis of pBS-sgE and pBS-sgI confirmed that no inadvertent mutations had occurred during PCR and cloning.

Construction of recombinant virus $FHV\text{-}gI\Delta C_1$. FHVΔgI-LZ has been described previously (38). In this mutant, the gI gene had been disrupted by replacing nt 203 to 923 with an expression cassette, consisting of the *lacZ* gene downstream of the encephalomyocarditis virus internal ribosomal entry site. To construct an FHV recombinant that expresses $gI\Delta C_1$, the Cys^{79}→Ser substitution was introduced into plasmid pUS1 (37), which contains a 7-kb *Eco*RV-*Bam*HI fragment spanning the genes for gD, gI, gE, US8.5, US9, US10, and US1 (56). To this end, the 292-bp *Pml*I-*Hin*dIII fragment of $pBS\text{-}gI\Delta M\Delta C_1$ was first inserted into *Pml*I- and *Hin*dIII-digested pBS-gI, resulting in $pBS\text{-}gI\Delta C_1$. Subsequently, the *Xho*I-*Bam*HI fragment from this plasmid was exchanged with the corresponding region in pUS1, yielding the transfer vector $pUS1\text{-}gI\Delta C_1$. Sequence analysis of the relevant region confirmed that $pUS1\text{-}gI\Delta C_1$ had the correct

nucleotide substitution and that no inadvertent mutations had been introduced during the cloning procedures.

To generate recombinant FHV-gIΔC_1, 10^6 CRFK cells, seeded in 35-mm-diameter dishes, were cotransfected with approximately 50 ng of FHVΔgI-LZ DNA and 1 μg of pUS1-gIΔC_1. The culture supernatants were harvested 7 days later, and plaque assays were performed. Recombinant viruses that had lost the encephalomyocarditis virus internal ribosomal entry site-*lacZ* expression cassette were identified by staining of plaques with X-Gal (5-bromo-4-chloro-3-indolyl-β-D-galactopyranoside; Boehringer Mannheim) as a substrate and were plaque purified three times prior to the preparation of virus stocks. Proper introduction of the mutation was confirmed by Southern blot hybridization and sequence analysis of viral DNA.

Transfection of vTF7-3-infected cells and metabolic labeling. Subconfluent monolayers of OST7-1 cells grown in 35-mm-diameter dishes were washed once with DMEM and infected with vaccinia virus vTF7-3 at a multiplicity of infection of 3 in DMEM at 37°C. One hour postinfection (p.i.), the cells were washed with DMEM and transfected with a mixture consisting of 2 to 5 μg of plasmid DNA, 500 μl of DMEM, and 10 μl of Lipofectin (Gibco BRL, Life Technologies, Inc.). After a 5-min incubation at room temperature, 500 μl of DMEM was added, and incubation was continued at 37°C. At 2 h p.i., the temperature was lowered to 32°C. From 4 to 5 h p.i., the cells were incubated with 1 ml of minimum essential medium with Earle's salts, lacking cysteine and methionine (Gibco BRL, Life Technologies, Inc.). Then, 100 μCi of Redivue L-[^{35}S] in vitro cell labeling mix ([^{35}S]Met plus [^{35}S]Cys; Amersham) was added to the culture medium and incubation was continued for 1 h. The cells were harvested either immediately or after a 2-h chase with DMEM–10% FCS containing 5 mM (each) L-methionine and L-cysteine.

Metabolic labeling of FHV-infected cells. Subconfluent monolayers of CRFK cells in 35-mm-diameter dishes were washed once with DMEM and infected with either wild-type FHV strain B927 or recombinant FHV at a multiplicity of infection of 5 at 37°C. At 1 h p.i., the culture medium was replaced by DMEM–10% FCS, and the incubation was continued at 37°C. Metabolic labeling was done as described for vTF7-3-infected cells, except that the cysteine-methionine depletion and subsequent labeling procedures were performed 2 h later and at 37°C, unless indicated otherwise.

RIPA and SDS-PAGE. Metabolically labeled cells were washed once with ice-cold phosphate-buffered saline and then lysed on ice in 600 μl of lysis buffer (20 mM Tris-Cl [pH 7.5], 1 mM EDTA, 100 mM NaCl, 1% Triton X-100) containing 1 μg of pepstatin A, 40 μg of aprotinin, and 1 μg of leupeptin per ml. For analysis under nonreducing conditions, the cells were washed with ice-cold phosphate-buffered saline containing 20 mM N-ethylmaleimide (NEM; Pierce) for 5 min and then lysed in lysis buffer supplemented with 20 mM NEM, in order to block free sulfhydryl groups. Nuclei and cell debris were removed by centrifugation for 1 min at 10,000 × *g* and 4°C. Two hundred microliters of the supernatant was mixed with 1 ml of detergent mix (50 mM Tris-Cl [pH 8.0], 62.5 mM EDTA, 0.4% sodium deoxycholate, 1% Nonidet P-40), and sodium dodecyl sulfate (SDS) was added to a final concentration of 0.25%. After 15 min on ice, the antisera were added (Cat-αFHV and Ra-αgE, 3 μl each; Ra-αgI, 5 μl) and incubation was continued for 16 h at 4°C. Immune complexes were collected by adding 50 μl of a 10% (wt/vol) suspension of formalin-fixed *Staphylococcus aureus* cells (Pansorbin; Calbiochem) in detergent mix. After a 30-min incubation at 4°C, the precipitates were washed three times with radioimmunoprecipitation assay (RIPA) buffer (10 mM Tris-Cl [pH 7.4], 150 mM NaCl, 0.1% SDS, 1% sodium deoxycholate, 1% Nonidet P-40). Digestion of immunoprecipitated proteins with peptide:N-glycosidase F (PNGase F; New England Biolabs) was performed in accordance with the instructions of the manufacturer but in the absence of reducing agents. Finally, the proteins were dissolved in 30 μl of modified Laemmli sample buffer (7) containing 5% β-mercaptoethanol (β-ME) unless indicated otherwise, heated for 5 min at 95°C, and analyzed by SDS-polyacrylamide gel electrophoresis (PAGE).

Purification and EndoLys-C digestion of secretory gI (sgI). vTF7-3-infected OST7-1 cells were transfected with pBS-sgE and either pBS-sgI or pBS-gIΔMΔC_1. Mock-transfected cells served as a negative control. Cells were depleted for cysteine from 4 to 5 h p.i.; [^{35}S]Cys (ICN) was then added to the tissue culture supernatant to a final concentration of 150 μCi/ml, and the cells were metabolically labeled from 5 to 8 h p.i. The culture supernatant was harvested, and detached cells and cell debris were removed by centrifugation at 12,000 × *g* for 2 min at 4°C. SDS was added to the supernatants to a final concentration of 1.3%; this was followed by a 15-min incubation at room temperature to dissociate gE-gI hetero-oligomers. Subsequently, the samples were diluted with detergent mix to an SDS concentration of 0.25%, and a standard RIPA with Ra-αgI serum was performed. Immune complexes were eluted from the formalin-fixed *S. aureus* cells with PNGase F buffer (50 mM sodium phosphate [pH 7.5], 0.5% SDS) and then treated with PNGase F. The reaction mixtures were diluted fivefold with distilled water and 10× endoproteinase Lys-C (EndoLys-C) buffer to end concentrations of 25 mM Tris-Cl (pH 8.5) and 1 mM EDTA. Proteolytic digestion was performed in a reaction volume of 250 μl at estimated enzyme/substrate ratios of 1:40 to 1:100 by adding 1.7 μg of rehydrated EndoLys-C (sequencing grade; Boehringer Mannheim). Incubation was for 14 h at 37°C. The digestion was stopped by adding 125 μl of modified Laemmli sample buffer (7) with or without 5% β-ME and then heating for 5 min at 95°C. The peptides were separated by using the discontinuous tricine-SDS-PAGE system developed by Schägger and von Jagow (47), with the separating gel containing 13.3% (wt/vol) glycerol and a monomer/cross-linker ratio of 16.5% T/6% C (where T denotes the total percentage of both acrylamide and bisacrylamide and C denotes the percentage concentration of the cross-linker relative to the total concentration T [see also reference 47]). Gels were run for 2 h at 30 V followed by 9 h at 30 mA, fixed for 30 min in 50% methanol–10% acetic acid, and vacuum dried at 80°C. Radiolabeled peptides were visualized by fluorography, using TranScreen phosphor screens (Kodak) in combination with Kodak BioMax MS films. The Rainbow ^{14}C-methylated protein low-molecular-weight marker (Amersham) was used to determine apparent molecular weights.

Plaque assays and immunohistochemistry. Plaque assays in CRFK cells, visualization of plaques by immunohistochemistry, and calculation of average plaque size have been described previously (37).

RESULTS

SDS-PAGE analysis of FHV gI under reducing and nonreducing conditions. The four cysteine residues in the ectodomain of FHV gI are located at positions 79 (C_1), 91 (C_2), 102 (C_3), and 223 (C_4) (Fig. 1). To determine whether they are involved in the formation of intra- and/or intermolecular disulfide bonds, gI was analyzed under reducing and nonreducing conditions. CRFK cells were infected with wild-type FHV strain B927 or, as a negative control, with the gI-deficient recombinant virus FHVΔgI-LZ (38). The cells were metabolically labeled from 7 to 8 h p.i. and lysed in the presence of 20 mM NEM to alkylate free sulfhydryl groups. The lysates were subjected to immunoprecipitation with a rabbit antiserum raised against residues 20 to 36 of FHV gI (Ra-αgI) (38), and the precipitated proteins were separated in SDS–7.5% polyacrylamide gels in the presence or absence of β-ME. In some experiments, the immunoprecipitates were treated with endoglycosidase H (EndoH) to distinguish immature gI (*i*gI) species from mature post-ER forms (data not shown). As reported previously (37, 38), under reducing conditions, *i*gI migrated as a 67,000-molecular-weight (67K) protein whereas mature gI (*m*gI) produced an EndoH-resistant 80 to 100K smear (Fig. 2, right panel, B927 −). When gI was analyzed under nonreducing conditions (Fig. 2, left panel, B927 −), three species were observed, one of which comigrated with reduced *i*gI. The other products, migrating at 60K and at 76 to 95K, apparently represent oxidized forms of *i*gI and *m*gI, respectively.

To facilitate the analysis of *m*gI, the immunoprecipitates were treated with PNGase F, an amidase which cleaves both high-mannose and hybrid as well as complex N-linked oligosaccharides. Reduced *i*gI was trimmed to 46 kDa, the expected size of the protein backbone, while reduced *m*gI was trimmed to yield a prominent 58-kDa species plus a number of minor products ranging from 56 to 62 kDa (Fig. 2, right panel, B927 +). The size difference between the PNGase F-treated *i*gI and *m*gI species is indicative of extensive post-ER modifications, which include O-glycosylation (38). The apparent size variation among PNGase F-treated *m*gI species presumably reflects heterogeneity in the number or composition of the O-glycans.

Analysis of the PNGase F-treated samples under nonreducing conditions revealed three major products (Fig. 2, left panel, B927 +). Two of these are *i*gI species, one virtually comigrating with the fully reduced protein (igI_{red}) and the other a faster-migrating oxidized form (igI_{ox}) running at 38K. The third product, migrating at 52K, represents oxidized *m*gI (mgI_{ox}). We did not detect products comigrating with fully reduced 58K *m*gI (mgI_{red}). A minor 41K *i*gI species was consistently found, but at present it is not clear whether it is a bona fide folding intermediate or a misfolded, aberrantly oxidized form. The data indicate that gI acquires at least one intramolecular disulfide bond. gI oligomers linked through intermolecular disulfide bonds were not detected.

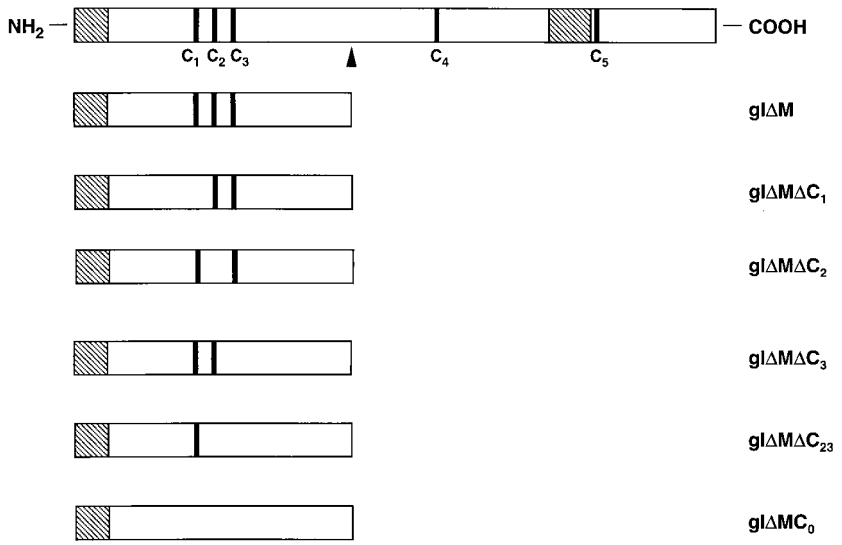

FIG. 1. Schematic representation of FHV gI, gIΔM, and the various gIΔM derivatives carrying Cys→Ser substitutions. The proteins are represented by open boxes. The N-terminal signal peptide and the transmembrane region of each protein are indicated by hatched boxes. C_1, C_2, C_3, and C_4, representing the cysteine residues in the ectodomain of gI at positions 79, 91, 102, and 223, respectively, are indicated by black bars. A fifth cysteine residue, C_5, present in the cytoplasmic domain at position 322, is also shown. The position of Arg^{166} is marked by an arrowhead.

The kinetics of disulfide bond formation and folding during FHV gI synthesis. To study the kinetics of disulfide bond formation and subsequent gI maturation, FHV-infected CRFK cells were pulse-labeled for 5 min at 8 h p.i. and then harvested either immediately or after chase periods of up to 120 min. Prior to analysis under reducing and nonreducing conditions, the immunoprecipitated gI species were treated with PNGase F. As shown in Fig. 3, *m*gI first appeared after a 30-min chase. Analysis under nonreducing conditions revealed that after a 5-min pulse-labeling, the majority of newly synthesized gI comigrated with $ig\mathrm{I}_{red}$ and thus was either fully reduced or had acquired intramolecular disulfide bonds that did not affect migration in SDS-polyacrylamide gels (Fig. 3, left panel, B927 0′). However, as determined by β-scanning, 25% of the labeled gI was already in the 38-kDa $ig\mathrm{I}_{ox}$ form. During the subsequent 10-min chase, the amount of $ig\mathrm{I}_{ox}$ increased to 60%. Thus, the conversion of $ig\mathrm{I}_{red}$ into $ig\mathrm{I}_{ox}$ occurred predominantly posttranslationally, with an estimated half-life ($t_{1/2}$) of 5 to 7 min. Subsequently, $ig\mathrm{I}_{ox}$ declined with an estimated $t_{1/2}$ of 35 min, concomitant with the appearance of $mg\mathrm{I}_{ox}$. The folding of gI appeared to be an inefficient process. After a 120-min chase, about 35% of gI still remained in the ER, and most of it comigrated with $ig\mathrm{I}_{red}$. Only 12% of the labeled gI appeared to have been converted into $mg\mathrm{I}_{ox}$.

C_2 and C_3 of gI are required for maturation of gE. We have previously shown that a gI derivative, gIΔM, which consists of

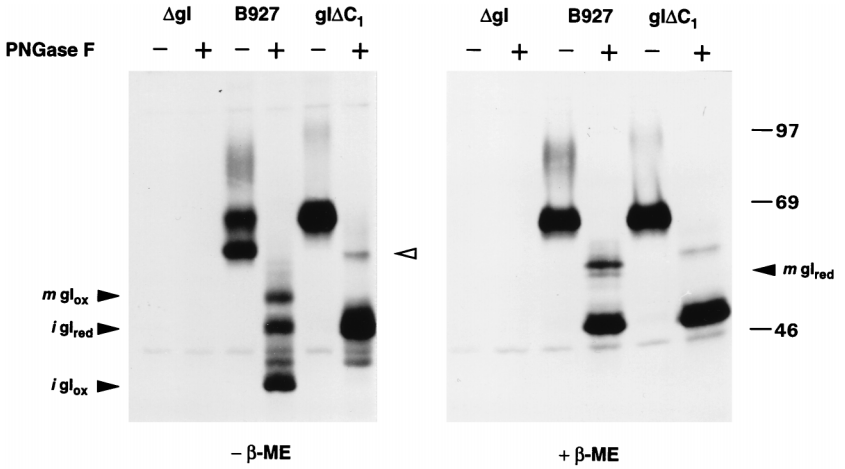

FIG. 2. Analysis of gI and $gI\Delta C_1$ under reducing and nonreducing conditions. Subconfluent monolayers of CRFK cells were infected with either wild-type FHV strain B927 (B927) or FHV-$gI\Delta C_1$ ($gI\Delta C_1$). Cells infected with the gI-deficient recombinant FHVΔgI-LZ (ΔgI) (38) served as a negative control. The cells were metabolically labeled from 7 to 8 h p.i. at 37°C. The cell lysates were prepared in the presence of 20 mM NEM to block free sulfhydryl groups and were then subjected to RIPA with the gI-specific antiserum Ra-αgI. The proteins were either treated with PNGase F (+) or mock treated (−) and separated in SDS–7.5% polyacrylamide gels in the absence and presence of β-ME (− β-ME and + β-ME, respectively). The closed arrowheads indicate immature reduced and oxidized gI species ($ig\mathrm{I}_{red}$ and $ig\mathrm{I}_{ox}$, respectively) and mature reduced and oxidized gI species ($mg\mathrm{I}_{red}$ and $mg\mathrm{I}_{ox}$, respectively). In the left-hand panel, mature $gI\Delta C_1$ is indicated by an open arrowhead. Molecular sizes are in kilodaltons.

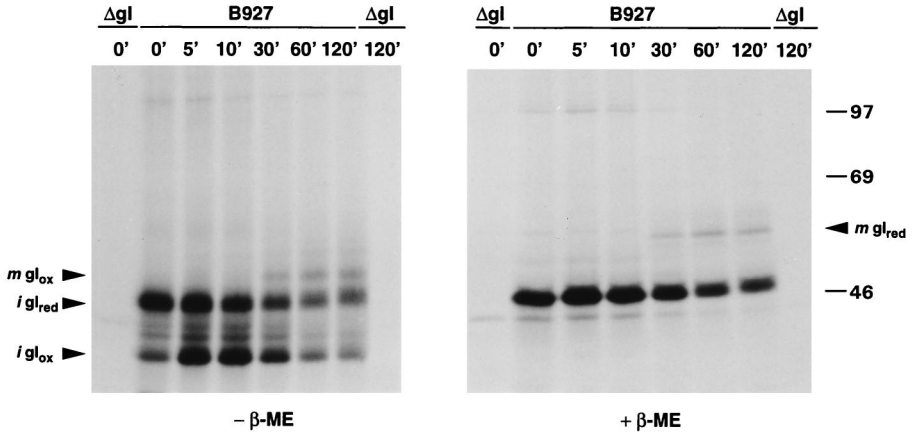

FIG. 3. Pulse-chase analysis of FHV gI under reducing and nonreducing conditions. Subconfluent monolayers of CRFK cells were infected with wild-type FHV strain B927 (B927). At 8 h p.i., the cells were metabolically labeled for 5 min at 37°C and harvested either immediately (0') or after chase periods of 5, 10, 30, 60, and 120 min (5', 10', 30', 60', and 120', respectively). To assure quantitative precipitation of labeled gI also after a 60-min or 120-min chase, the amount of unlabeled gI was reduced by adding 0.5 mM cycloheximide to the culture supernatant 30 min after labeling. Cells infected with FHVΔgI-LZ (ΔgI) and harvested after a 5-min pulse-labeling (0') or following a subsequent 120-min chase period (120') served as negative controls. Cell lysates, prepared in the presence of 20 mM NEM, were subjected to RIPA with Ra-αgI. To facilitate the analysis, all samples were treated with PNGase F. The proteins were separated in SDS–7.5% polyacrylamide gels in the absence (−) and presence (+) of β-ME. Immature reduced and immature oxidized gI species (igI_{red} and igI_{ox}, respectively) and mature reduced and mature oxidized gI species (mgI_{red} and mgI_{ox}, respectively) are indicated. Molecular sizes are in kilodaltons.

only the N-terminal 166 residues and thus lacks C_4, still induces gE maturation (37). Apparently, the formation of an intramolecular disulfide bridge involving C_4 is not essential for the interaction with gE or for ER-to-Golgi transport of the resulting complex. To study the role of the remaining cysteine residues, gIΔM derivatives in which C_1, C_2, or C_3 was replaced by Ser were constructed. These mutant proteins were coexpressed with gE in the vaccinia virus-based vTF7-3 expression system (21) and metabolically labeled for 1 h, followed by a 2-h chase. Immunoprecipitation was performed with an FHV-specific feline hyperimmune serum, Cat-αFHV. Conversion of the immature ER-resident 83K gE species into the mature 95K form was interpreted to indicate the assembly of a transport-competent gE-gIΔM hetero-oligomer (37). As shown in Fig. 4, substitution of C_1, as in $gI\Delta M\Delta C_1$, did not affect gE maturation. Thus, C_1, like C_4, is not essential for this process. In contrast, $gI\Delta M\Delta C_2$, $gI\Delta M\Delta C_3$, and $gI\Delta M\Delta C_{23}$, in which C_2 and/or C_3 had been replaced, and $gI\Delta MC_0$, which lacks all cysteine residues, failed to induce maturation of gE. Immunoprecipitation with the Ra-αgI antiserum confirmed that the gIΔM derivatives had been expressed to similar extents. Moreover, immature gE was found to coprecipitate with $gI\Delta M\Delta C_2$, $gI\Delta M\Delta C_3$, and $gI\Delta M\Delta C_{23}$, while in the reciprocal experiment, with a monospecific antiserum against gE, coprecipitation of the gIΔM derivatives was observed (data not shown). Apparently, replacement of C_2 and/or C_3 does not prevent the formation of the gE-gIΔM hetero-oligomer. However, the resulting complex is no longer transport competent and is retained in the ER. These observations fit a model for the disulfide-bonded structure of gI in which C_2 and C_3 as well as C_1 and C_4 form intramolecular disulfide bridges and in which the C_2-C_3 bond (but not the C_1-C_4 bond) is essential for ER-to-Golgi transport of the gE-gI hetero-oligomer.

Biochemical evidence for a C_1-C_4 disulfide bond. To test our hypothesis that C_1 and C_4 form a disulfide bridge, we followed a strategy entailing proteolytic digestion of purified radiolabeled gI and analysis of the resulting peptides under reducing and nonreducing conditions. To this end, secretory forms of gI (sgI) and gE (sgE), truncated immediately N terminal of their predicted transmembrane regions, were coexpressed in the vTF7-3 expression system. Pilot experiments had shown that sgE and sgI, when expressed separately, are retained in the cell. However, when coexpressed, they form a complex which is secreted into the culture supernatant (39), thus providing a source of mature gI virtually devoid of immature forms that could complicate the analysis. Cells, mock transfected or cotransfected to express $gI\Delta M\Delta C_1$ and sgE, were used as controls. The proteins were metabolically labeled with [^{35}S]Cys, the tissue culture supernatant was harvested, and the sgE-sgI complex was dissociated with SDS. RIPA was performed with the Cat-αFHV and Ra-αgI antisera; this was followed by PNGase F digestion to remove N-glycans. PNGase F-treated mature sgE and sgI migrate at 53K and 44K, respectively, in SDS-polyacrylamide gels, whereas their immature deglycosylated forms run at 44K and 34K, respectively (39). The size differences between the intracellular and secreted forms indicate that the truncated proteins are posttranslationally modified to extents similar to those of full-length gE and gI. As shown in Fig. 5a, the Cat-αFHV serum predominantly detected mature sgE whereas the Ra-αgI serum readily precipitated both sgI and the 17K $gI\Delta M\Delta C_1$ product (Fig. 5a, left panel). Under nonreducing conditions (Fig. 5a, right panel),

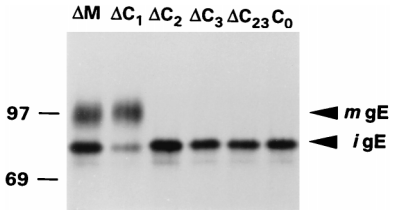

FIG. 4. Coexpression of gE with cysteine mutants of gIΔM. vTF7-3-infected OST7-1 cells were cotransfected with plasmid pBS-gE and a plasmid encoding gIΔM or one of its derivatives ($gI\Delta M\Delta C_1$, $-\Delta C_2$, $-\Delta C_3$, $-\Delta C_{23}$, or $-C_0$). The cells were metabolically labeled from 5 to 6 h p.i., followed by a 2-h chase. The cell lysates were subjected to RIPA with an FHV-specific feline hyperimmune serum, Cat-αFHV. The samples were analyzed in SDS–7.5% polyacrylamide gels. The immature, EndoH-sensitive 83-kDa gE species (*ig*E) and the mature, EndoH-resistant, 95-kDa gE species (*m*gE) are indicated with arrowheads. Molecular sizes are in kilodaltons.

sgI migrated at 38K and thus showed a 6K shift in apparent molecular weight, identical to that of full-length gI (Fig. 2).

Immunoprecipitated PNGase F-treated sgI and gIΔMΔC_1 were digested with EndoLys-C. In the case of sgI, this should yield radiolabeled peptides of 63, 24, and 50 residues, the latter containing two potential O-glycosylation sites (Fig. 5b). Glycosylation at these sites would result in an increase in apparent molecular weight of approximately 4,000, and the product would be expected to run either as a diffuse smear or as a set of multiple bands in SDS-polyacrylamide gels. Digestion of gIΔMΔC_1 should yield only the 24-residue peptide containing C_2 and C_3. The sgI and gIΔMΔC_1 digests were separated in polyacrylamide gels (16.5% T, 6% C), employing the discontinuous tricine-SDS-PAGE system developed by Schägger and von Jagow (47), and radiolabeled peptides were visualized by fluorography. As shown in Fig. 5c, analysis of the sgI digest under reducing conditions yielded two distinct products of 3K and 5.5K plus a family of products migrating at 8 to 9K. The 5.5K and 8 to 9K peptides were absent from the mock-transfected cells and the gIΔMΔC_1 digest, but the latter did contain the 3K peptide. This product was thus identified as the 24-residue fragment containing C_2 and C_3. The 5.5K and 8 to 9K products apparently represent the unglycosylated 63-residue fragment containing C_1 and the O-glycosylated 50-residue fragment containing C_4, respectively. Under nonreducing conditions, the 3K peptide did not show a shift up in apparent molecular weight, indicating that it is not disulfide linked to other peptides (Fig. 5c, right panel, sgI). The 5.5 and 8K to 9K products, however, appear to be disulfide bonded, since they both were absent under nonreducing conditions and were replaced by a 16K product. These findings indicate that residues C_1 and C_4 form an intramolecular disulfide bridge.

Under both reducing and nonreducing conditions, a minor 8K peptide was detected in the gIΔMΔC_1 digest. This may represent a partial digestion product or, more likely, a digestion product of the high-molecular-weight polypeptide contaminating the gIΔMΔC_1 immunoprecipitate (Fig. 5a).

Characterization of a recombinant FHV expressing gIΔC_1. The experiments described above suggest that the C_1-C_4 bond is not essential for the formation of the gE-gI complex or for its release from the ER. However, since C_1 and C_4 are conserved in all gI proteins characterized thus far, these residues could be important for gE-gI function. To study this, an FHV recombinant, FHV-gIΔC_1, was constructed in which C_1 of gI was replaced by Ser. The biosynthesis of gIΔC_1 differed from that of wild-type gI in several respects. Under nonreducing conditions, *i*gI_{ox} and *m*gI_{ox} forms were absent (Fig. 2, left panel) and *i*gIΔC_1 and *m*gIΔC_1 virtually comigrated with their respective fully reduced forms (Fig. 2, right panel). Furthermore, *m*gIΔC_1 was considerably larger than *m*gI (85 to 115K instead of 80 to 100K; see also Fig. 6a). PNGase F treatment suggested that this size increase could be attributed to a more extensive processing of N-linked glycans. However, since PNGase F-treated *m*gIΔC_1 was still 2K larger than *m*gI (Fig. 2, right panel), substitution of C_1 apparently also affected O-glycosylation. The more elaborate posttranslational processing of gIΔC_1 was not temperature dependent and occurred also at 32 and 39°C (Fig. 6a).

As anticipated, gE still matured in FHV-gIΔC_1-infected cells, but maturation was less efficient than in cells infected with wild-type FHV strain B927 (Fig. 6b). Interestingly, this effect was most pronounced at 32°C. Apparently, the C_1→S substitution in gI results in a conditional cold-sensitivity defect affecting either the formation or subsequent ER-to-Golgi transport of gE-gI.

To determine whether substitution of C_1 affected the func-

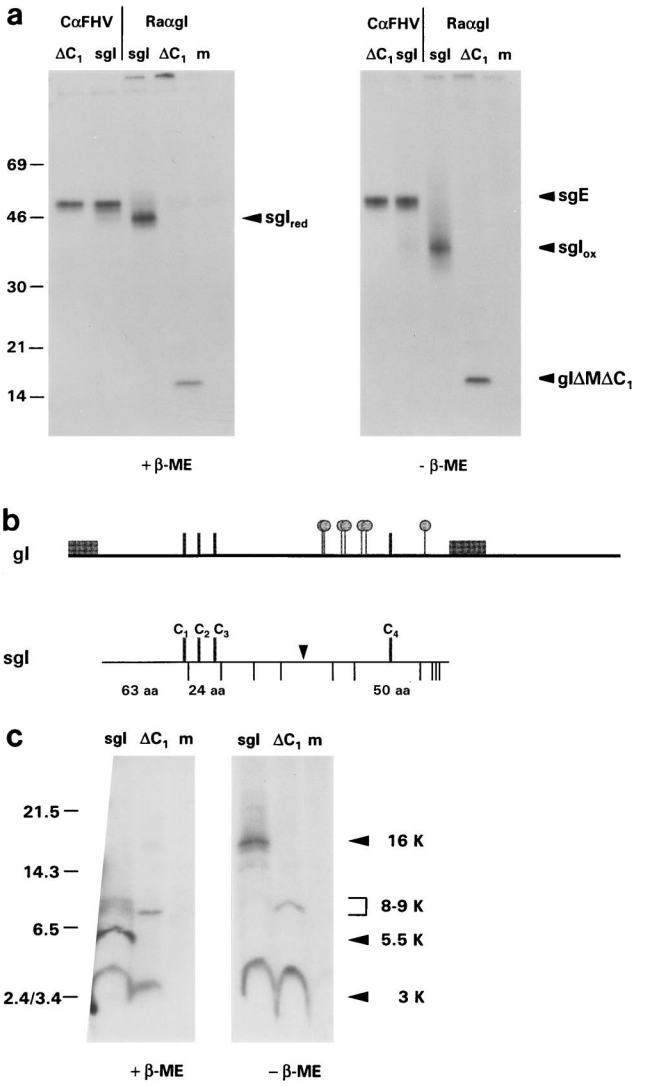

FIG. 5. Protein-chemical analysis of the disulfide-bonded structure of FHV gI. (a) Secretory forms of gE and gI (sgI) were coexpressed in vTF7-3-infected OST7-1 cells. Mock-transfected cells (m) and cells coexpressing gIΔMΔC_1 and gE (ΔC_1) were used as controls. The cells were metabolically labeled with [^{35}S]Cys from 5 to 8 h p.i. The culture supernatants were harvested, treated with SDS to dissociate the sgE-sgI hetero-oligomers, and subjected to RIPA with either Cat-αFHV (CαFHV) or Ra-αgI (RaαgI). N-linked oligosaccharides were removed by treating the immunoprecipitates with PNGase F. The samples were analyzed in SDS–15% polyacrylamide gels in the presence (+) or absence (−) of β-ME. Of each Ra-αgI precipitate, only one-quarter was analyzed; the remainder was digested with EndoLys-C (see below). Mature reduced and oxidized sgI (sgI_{red} and sgI_{ox}, respectively), mature sgE (sgE), and gIΔMΔC_1 are all indicated. (b) The EndoLys-C restriction map of sgI. The upper panel shows a schematic representation of full-length gI. The signal peptide and the transmembrane anchor are indicated by hatched boxes, the cysteine residues in the ectodomain (C_1 to C_4) are indicated by black bars, and potential O-glycosylation sites are indicated by "lollipops." The lower panel shows a schematic representation of sgI. The protein is depicted as a horizontal bar, and the relative positions of the four cysteine residues and Arg^{166} (arrowhead) are indicated. EndoLys-C cuts C terminal to lysine residues. The positions of these residues in sgI are marked by vertical lines below the horizontal bar. The predicted sizes of the fragments containing C_1 to C_4 are given in amino acids (aa). (c) Schägger-von Jagow SDS-PAGE analysis of EndoLys-C-generated radiolabeled peptides. Immunoprecipitated, PNGase F-treated sgI and gIΔMΔC_1 (see panel a) were digested with EndoLys-C (sgI and ΔC_1, respectively). Material immunoprecipitated from mock-infected cells was used as a control (m). The samples were analyzed under reducing (+ β-ME) and nonreducing (− β-ME) conditions in 16.5% T–6% C polyacrylamide gels, employing the discontinuous tricine-SDS-PAGE system (47). Radiolabeled peptides were visualized by fluorography. The sgI-derived peptides are indicated at the right. Peptide sizes were estimated by using the Rainbow low-molecular-weight marker (Amersham). Molecular sizes are in kilodaltons.

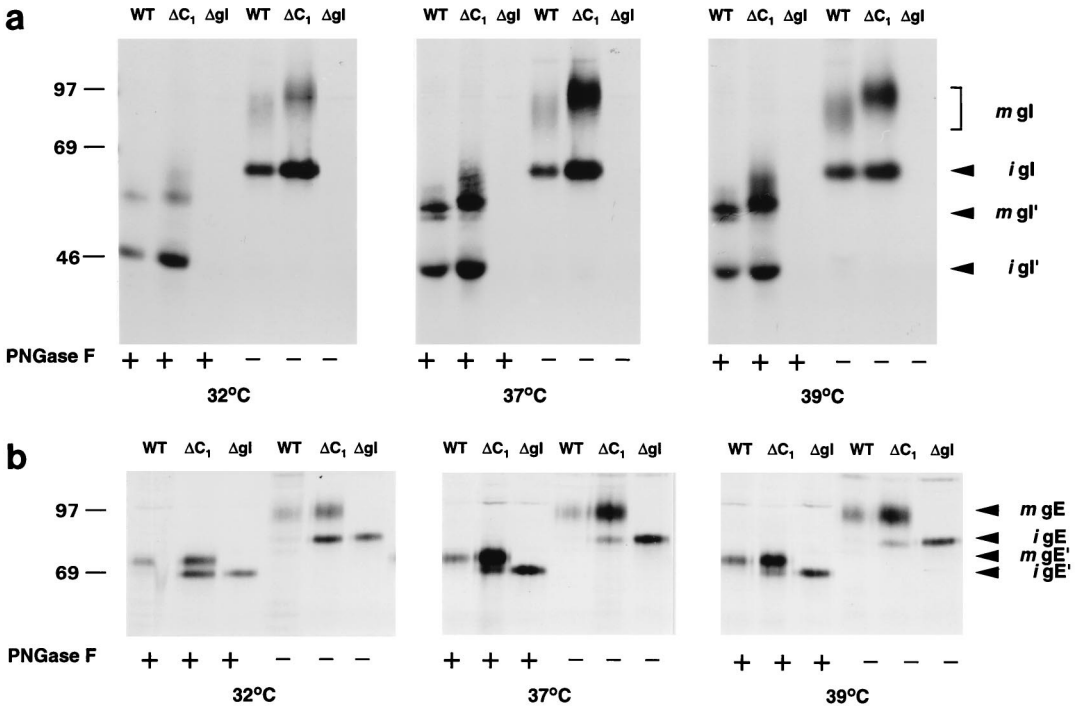

FIG. 6. Biosynthesis of gE and gI in FHV-gIΔC_1-infected cells. (a) Comparative analysis of gIΔC_1. Subconfluent monolayers of CRFK cells were infected at 37°C with wild-type FHV strain B927 (WT), with FHV-gIΔC_1 (ΔC_1), or with FHVΔgI-LZ (ΔgI). The cells were metabolically labeled from 7 to 8 h p.i. at 32, 37, or 39°C. Following a 2-h chase period at the respective temperatures, the cells were harvested and the cell lysates were subjected to RIPA with Ra-αgI. The proteins were treated with PNGase F (+) or mock treated (−) and subsequently analyzed in SDS–7.5% polyacrylamide gels. The immature and mature gI forms are indicated (*i*gI and *m*gI, respectively), as are the corresponding PNGase F-treated species (*i*gI′ and *m*gI′, respectively). (b) Maturation of gE in FHV-gIΔC_1-infected cells. The experiment was performed as described above, except that RIPA was done with the gE-specific antiserum, Ra-αgE. The immature and mature gE forms are indicated (*i*gE and *m*gE, respectively), as are the corresponding PNGase F-treated species (*i*gE′ and *m*gE′, respectively). Molecular sizes are in kilodaltons.

tion of gE-gI, the plaque size of FHV gIΔC_1 was compared to that of the wild-type virus. The gI-deficient recombinant FHVΔgI-LZ served as a control. Plaque assays were performed in CRFK cells at 32, 37, and 39°C. Plaques were visualized immunohistochemically, and average plaque sizes were determined in square millimeters (Fig. 7). Whereas FHVΔgI-LZ displayed a small-plaque phenotype at all three temperatures, the average plaque size of FHV-gIΔC_1 equaled that of the wild-type strain B927. Apparently, elimination of the C_1-C_4 bond does not affect the function of gE-gI in vitro.

DISCUSSION

Alphaherpesvirus gE and gI constitute important virulence factors (8, 11, 12, 18, 27, 28, 40, 44, 48, 50, 53, 55), apparently promoting cell-to-cell transmission in mucosal and neuronal tissues (4, 10–12, 49, 60). In infected cells, gE and gI form a noncovalently linked hetero-oligomer (23, 38, 53, 54, 58, 61), and it is assumed that this complex, expressed at the cell surface, represents the functional unit. For release from the ER and transport along the exocytotic route, FHV gE must oligomerize with gI (38). Complex formation and subsequent maturation of the proteins thus provide convenient parameters by which to assess different aspects of the fate and function of either glycoprotein (37).

In the present study, we probed the disulfide-bonded structure of gI by employing single and pairwise substitutions of the four cysteine residues in the ectodomain of FHV gI. The resulting mutant proteins were coexpressed with gE in the vTF7-3 system (21), and the effect on gE-gI interaction and gE maturation was monitored. We found that gI derivatives lacking C_1 and/or C_4 assembled into a transport-competent complex with gE. In contrast, derivatives lacking C_2 and/or C_3 still bound to gE but the hetero-oligomer was retained in the ER. In addition, we took a protein-chemical approach and performed an endoproteolytic digestion of a [^{35}S]Cys-labeled secretory form of gI followed by PAGE analysis of the radiolabeled peptides under reducing and nonreducing conditions.

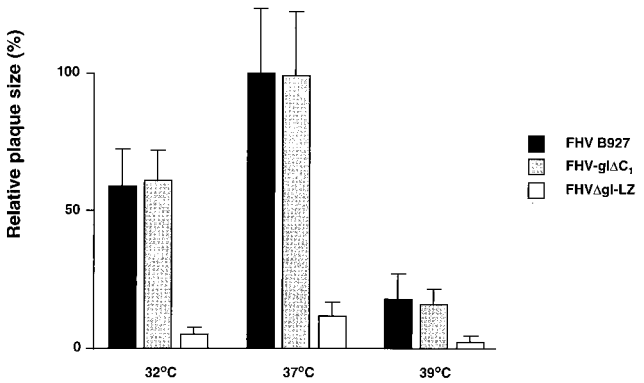

FIG. 7. Plaque phenotype of FHV-gIΔC_1. A plaque assay was performed by infecting CRFK cells at 37°C with FHV B927, FHV-gIΔC_1, or FHVΔgI-LZ and then incubating for 72 h at 32, 37, or 39°C. Plaques were visualized immunohistochemically, and plaque sizes were quantitated by measuring 25 randomly selected plaques along the *x* and *y* axes at a 20-fold magnification. The average plaque size in square millimeters was then calculated from the mean radius (*r*) by using the term πr^2. The histogram shows the plaque sizes relative to that of FHV B927 incubated at 37°C. Standard deviations are indicated by bars. The experiment was performed three times, yielding essentially identical results.

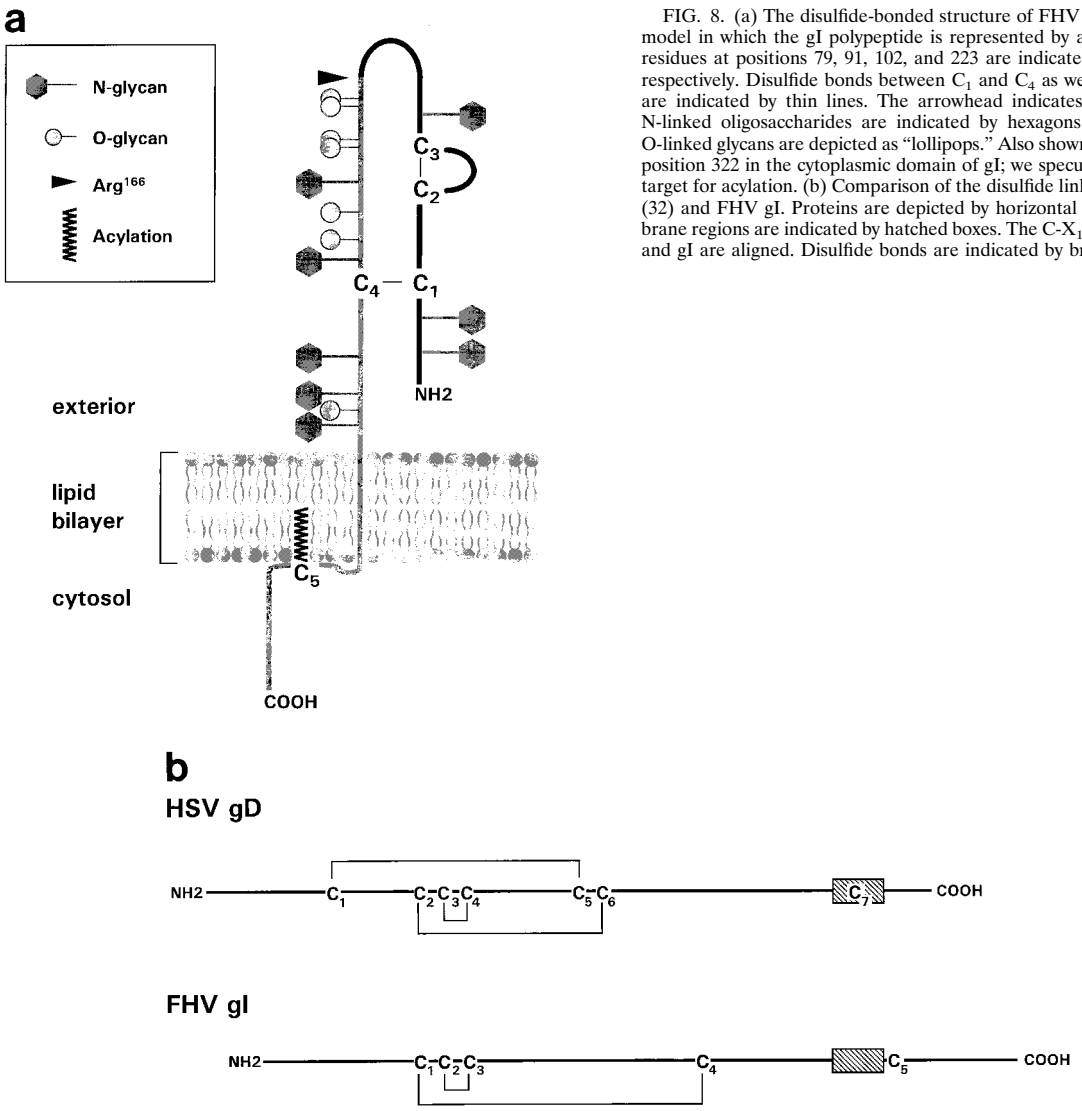

FIG. 8. (a) The disulfide-bonded structure of FHV gI. Shown is a schematic model in which the gI polypeptide is represented by a thick line. The cysteine residues at positions 79, 91, 102, and 223 are indicated by C_1, C_2, C_3, and C_4, respectively. Disulfide bonds between C_1 and C_4 as well as between C_2 and C_3 are indicated by thin lines. The arrowhead indicates the position of Arg^{166}. N-linked oligosaccharides are indicated by hexagons on sticks, and putative O-linked glycans are depicted as "lollipops." Also shown is cysteine residue C_5 at position 322 in the cytoplasmic domain of gI; we speculate that this residue is a target for acylation. (b) Comparison of the disulfide linkage patterns of HSV gD (32) and FHV gI. Proteins are depicted by horizontal bars, and the transmembrane regions are indicated by hatched boxes. The $C\text{-}X_{11}\text{-}C\text{-}X_{8-10}\text{-}C$ motifs in gD and gI are aligned. Disulfide bonds are indicated by brackets.

Radiolabeled EndoLys-C-generated peptide species of 5K and 8 to 9K, predicted to contain C_1 and C_4, respectively, were found to be disulfide bonded. However, a 3K peptide, identified to contain both C_2 and C_3, was not disulfide linked to any other peptide. The biological properties of the cysteine mutants, in combination with the direct protein-chemical evidence for the C_1-C_4 bond, led us to a model for gI in which C_1 and C_4 as well as C_2 and C_3 form intramolecular disulfide bridges (Fig. 8a). Since the cysteines in the ectodomain of gI proteins have been conserved during alphaherpesvirus divergence (2, 29, 34, 39), we predict that this model applies for all gI proteins.

In FHV-infected cells, the disulfide-bonded gI structure is generated posttranslationally, at least in part. Newly synthesized gI is converted into an immature, EndoH-sensitive oxidized form, $ig\mathrm{I}_{ox}$. The formation of $ig\mathrm{I}_{ox}$ can be followed under nonreducing conditions in SDS-polyacrylamide gels since it is accompanied by a 6K decrease in apparent molecular weight. Comparative analysis of the recombinant virus FHV-gIΔC_1, which carries a $C_1 \rightarrow S$ substitution, indicated that this shift in mobility is due to the formation of the C_1-C_4 bridge. It is of note that we did not obtain gel electrophoretic evidence of a disulfide bond between C_2 and C_3. However, closure of this bond would produce a loop of only 10 residues, which might not appreciably affect migration in SDS-polyacrylamide gels.

C_1-C_4 disulfide bond formation occurs with an estimated $t_{1/2}$ of 5 to 7 min. In comparison, the release of gI from the ER is slow, occurring with an estimated $t_{1/2}$ of 35 min. Also, gI folding appears to be an inefficient process: of the molecules synthesized during a 5-min pulse, more than 35% were still in the ER after a 120-min chase, as determined by β-scanning. Most had not even acquired the C_1-C_4 bond and might represent irretrievably misfolded gI species. Only some 12% of the FHV gI acquired EndoH resistance. This estimate, however, should be regarded with caution, since mature gI may not have been quantitatively detected due to a different avidity of the Ra-αgI serum for immature gI (38), to a loss of gI following incorporation into secreted virions, and to the extensive and heterogeneous posttranslational modifications which cause *m*gI to migrate as a diffuse smear in SDS-polyacrylamide gels. Our results are consistent with observations made for PRV (53) and bovine herpesvirus (54). In cells infected by these viruses, significant amounts of gI are also retained in the ER and not recruited into transport-competent hetero-oligomeric complexes.

Elimination of the C_1-C_4 disulfide bond, as in gIΔC_1, affected the posttranslational modification of gI, leading to an even more exuberant processing of N-linked glycans and possibly also to the addition of an extra O-linked oligosaccharide. These observations are not without precedent. Hyperglycosylation is also observed when gI is expressed in the absence of gE and vice versa (38, 58). Furthermore, it was recently reported that the elimination of a disulfide bond in the hemagglutinin-neuraminidase glycoprotein of Newcastle disease virus resulted in the usage of a normally inaccessible N-linked glycosylation site (35). Apparently, both the oligosaccharide chains and potential O-glycosylation sites of gIΔC_1 are more accessible to glycosyltransferases and other sugar-modifying enzymes than those of wild-type gI. We cannot exclude the possibility, however, that in gIΔC_1 an additional O-glycosylation site was created inadvertently by replacing C_1 with a Ser residue.

Analysis of FHV-gIΔC_1 confirmed the results of our heterologous expression studies in that C_1, and thus the formation of the C_1-C_4 bond, was found to be dispensable for intracellular transport of the gE-gI hetero-oligomer. Because disruption of disulfide bonds often results in a temperature-sensitive phenotype (31), we studied gE biosynthesis at 32, 37, and 39°C. At 32°C, the efficiency of gE maturation in FHV-gIΔC_1-infected cells was indeed significantly reduced compared to that in wild-type FHV-infected cells. Apparently, this defect could be overcome at the elevated temperatures. Perhaps the C_1-C_4 bond facilitates the occurrence of a thermodynamically unfavorable conformational change in gE and/or gI that is essential for ER-to-Golgi apparatus transport of the complex.

Alphaherpesviruses lacking gE and/or gI generally display a small-plaque phenotype (4, 11, 36, 37, 41, 48, 54, 60). We have previously shown that deletion of the gI gene from the FHV genome results in a 85% reduction in plaque size in CRFK cells compared to that of the parental wild-type FHV strain B927. FHV recombinants expressing mutant gI proteins produce plaques of intermediate size (37). Quantitation of plaque size thus provides an easy and useful assay by which to assess gE-gI function in vitro (33, 37, 52). Despite the low overall level of amino acid sequence identity among gI proteins of different alphaherpesvirus species, which is on the order of 20 to 30% and is mainly restricted to the N-terminal half of the ectodomain, the cysteine residues are strictly conserved (2, 29, 34, 39). It was thus anticipated that disruption of the C_1-C_4 disulfide bond would affect the function of gE-gI. Surprisingly, however, the plaques of FHV-gIΔC_1 were indistinguishable from those of the wild-type strain B927 at 39, 37, and 32°C. We conclude that C_1 and the formation of the C_1-C_4 bond are not essential for gE-gI-mediated cell-to-cell spread in vitro. Why, then, have C_1 and C_4 been conserved? One obvious explanation is that the loss of the C_1-C_4 bond would interfere with efficient viral spread during natural infection. Alternatively, disruption of the C_1-C_4 bond may affect the stability of the gE-gI complex, making it more vulnerable to proteolytic degradation in vivo, or may increase its antigenicity. In all of these cases, the loss of the C_1-C_4 bond would result in a decrease in viral fitness.

The presence of a characteristic cysteine motif, C-X_{11}-C-X_{8-10}-C, in the ectodomains of gG, gD, and gI has been interpreted to indicate that these glycoproteins have arisen through gene duplication (34). The ectodomain of gD contains six cysteine residues, with C_2, C_3, and C_4 apparently corresponding to C_1, C_2, and C_3 of gI (34). For gD of HSV types 1 and 2, the disulfide-bonded structure has been resolved. Disulfide bridges are formed between C_1 and C_5, C_2 and C_6, and C_3 and C_4 (Fig. 8b) (32). As predicted by Long et al. (32), the disulfide-bonded structure of gI, as determined in this paper, conforms to that of gD. Interestingly, of the three disulfide bridges in HSV gD, the C_1-C_5 bond—i.e., the one apparently absent from gI—is the least important for function (32). Our results are consistent with McGeoch's hypothesis that gD and gI are derived from a common ancestral protein (34). However, the question of whether these proteins are indeed evolutionarily related can be answered only by a comparison of their three-dimensional structures.

ACKNOWLEDGMENTS

We thank D. Harbour and B. Moss for providing the virus stocks of FHV strain B927 and vTF7-3, respectively, and A. de Vries and H. Lenstra for stimulating discussions.

J. D. F. Mijnes was supported by Rhône Mérieux, Lyon, France. The research of R. J. de Groot was made possible by a fellowship from the Royal Netherlands Academy for Sciences and Arts.

REFERENCES

1. **Alconada, A., U. Bauer, and B. Hoflack.** 1996. A tyrosine-based motif and a casein kinase II phosphorylation site regulate the intracellular trafficking of the varicella-zoster virus glycoprotein I, a protein localized in the trans-Golgi network. EMBO J. **15:**6096–6110.
2. **Audonnet, J. C., J. Winslow, G. Allen, and E. Paoletti.** 1990. Equine herpesvirus type 1 unique short fragment encodes glycoproteins with homology to herpes simplex virus type 1 gD, gI and gE. J. Gen. Virol. **71:**2969–2978.
3. **Ausubel, F. M., R. Brent, R. E. Kingston, D. D. Moore, J. G. Seidman, J. A. Smith, and K. Struhl (ed.).** 1989. Current protocols in molecular biology. Greene Publishing Associates and Wiley-Interscience, New York, N.Y.
4. **Balan, P., N. Davis Poynter, S. Bell, H. Atkinson, H. Browne, and T. Minson.** 1994. An analysis of the in vitro and in vivo phenotypes of mutants of herpes simplex virus type 1 lacking glycoproteins gG, gE, gI or the putative gJ. J. Gen. Virol. **75:**1245–1258.
5. **Baucke, R. B., and P. G. Spear.** 1979. Membrane proteins specified by herpes simplex viruses. V. Identification of an Fc-binding glycoprotein. J. Virol. **32:**779–789.
6. **Bell, S., M. Cranage, L. Borysiewicz, and T. Minson.** 1990. Induction of immunoglobulin G Fc receptors by recombinant vaccinia viruses expressing glycoproteins E and I of herpes simplex virus type 1. J. Virol. **64:**2181–2186.
7. **Cannon-Carlson, S., and J. Tang.** 1997. Modification of the Laemmli sodium dodecyl sulfate-polyacrylamide gel electrophoresis procedure to eliminate artifacts on reducing and nonreducing gels. Anal. Biochem. **246:**146–148.
8. **Card, J. P., M. E. Whealy, A. K. Robbins, and L. W. Enquist.** 1992. Pseudorabies virus envelope glycoprotein gI influences both neurotropism and virulence during infection of the rat visual system. J. Virol. **66:**3032–3041.
9. **Crandell, R. A., C. G. Fabricant, and W. A. Nelson-Rees.** 1973. Development, characterization, and viral susceptibility of a feline (*Felis catus*) renal cell line (CRFK). In Vitro **9:**176–185.
10. **Davis-Poynter, N., S. Bell, T. Minson, and H. Browne.** 1994. Analysis of the contributions of herpes simplex virus type 1 membrane proteins to the induction of cell-cell fusion. J. Virol. **68:**7586–7590.
11. **Dingwell, K. S., C. R. Brunetti, R. L. Hendricks, Q. Tang, M. Tang, A. J. Rainbow, and D. C. Johnson.** 1994. Herpes simplex virus glycoproteins E and I facilitate cell-to-cell spread in vivo and across junctions of cultured cells. J. Virol. **68:**834–845.
12. **Dingwell, K. S., L. C. Doering, and D. C. Johnson.** 1995. Glycoproteins E and I facilitate neuron-to-neuron spread of herpes simplex virus. J. Virol. **69:**7087–7098.
13. **Dubin, G., I. Frank, and H. M. Friedman.** 1990. Herpes simplex virus type 1 encodes two Fc receptors which have different binding characteristics for monomeric immunoglobulin G (IgG) and IgG complexes. J. Virol. **64:**2725–2731.
14. **Dubin, G., E. Socolof, I. Frank, and H. M. Friedman.** 1991. Herpes simplex virus type 1 Fc receptor protects infected cells from antibody-dependent cellular cytotoxicity. J. Virol. **65:**7046–7050.
15. **Edson, C. M.** 1993. Phosphorylation of neurotropic alphaherpesvirus envelope glycoproteins: herpes simplex virus type 2 gE2 and pseudorabies virus gI. Virology **195:**268–270.
16. **Edson, C. M.** 1993. Tyrosine sulfation of varicella-zoster virus envelope glycoprotein gpI. Virology **197:**159–165.
17. **Elroy-Stein, O., and B. Moss.** 1990. Cytoplasmic expression system based on constitutive synthesis of bacteriophage T7 RNA polymerase in mammalian cells. Proc. Natl. Acad. Sci. USA **87:**6743–6747.
18. **Enquist, L. W., J. Dubin, M. E. Whealy, and J. P. Card.** 1994. Complementation analysis of pseudorabies virus gE and gI mutants in retinal ganglion cell neurotropism. J. Virol. **68:**5275–5279.
19. **Favoreel, H. W., H. J. Nauwynck, P. Van Oostveldt, T. C. Mettenleiter, and M. B. Pensaert.** 1997. Antibody-induced and cytoskeleton-mediated redis-

tribution and shedding of viral glycoproteins, expressed on pseudorabies virus-infected cells. J. Virol. **71:**8254–8261.
20. **Frank, I., and H. M. Friedman.** 1989. A novel function of the herpes simplex virus type 1 Fc receptor: participation in bipolar bridging of antiviral immunoglobulin G. J. Virol. **63:**4479–4488.
21. **Fuerst, T. R., E. G. Niles, F. W. Studier, and B. Moss.** 1986. Eukaryotic transient-expression system based on recombinant vaccinia virus that synthesizes bacteriophage T7 RNA polymerase. Proc. Natl. Acad. Sci. USA **83:** 8122–8126.
22. **Gaskell, R. M., and R. C. Povey.** 1979. The dose response of cats to experimental infection with feline viral rhinotracheitis virus. J. Comp. Pathol. **89:** 179–191.
23. **Johnson, D. C., and V. Feenstra.** 1987. Identification of a novel herpes simplex virus type 1-induced glycoprotein which complexes with gE and binds immunoglobulin. J. Virol. **61:**2208–2216.
24. **Johnson, D. C., M. C. Frame, M. W. Ligas, A. M. Cross, and N. D. Stow.** 1988. Herpes simplex virus immunoglobulin G Fc receptor activity depends on a complex of two viral glycoproteins, gE and gI. J. Virol. **62:**1347–1354.
25. **Kimura, H., S. E. Straus, and R. K. Williams.** 1997. Varicella-zoster virus glycoproteins E and I expressed in insect cells form a heterodimer that requires the N-terminal domain of glycoprotein I. Virology **233:**382–391.
26. **Knapp, A. C., and L. W. Enquist.** 1997. Pseudorabies virus recombinants expressing functional virulence determinants gE and gI from bovine herpesvirus 1.1. J. Virol. **71:**2731–2739.
27. **Kritas, S. K., M. B. Pensaert, and T. C. Mettenleiter.** 1994. Invasion and spread of single glycoprotein deleted mutants of Aujeszky's disease virus (ADV) in the trigeminal nervous pathway of pigs after intranasal inoculation. Vet. Microbiol. **40:**323–334.
28. **Kritas, S. K., M. B. Pensaert, and T. C. Mettenleiter.** 1994. Role of envelope glycoproteins gI, gp63 and gIII in the invasion and spread of Aujeszky's disease virus in the olfactory nervous pathway of the pig. J. Gen. Virol. **75:** 2319–2327.
29. **Leung-Tack, P., J. C. Audonnet, and M. Rivière.** 1994. The complete DNA sequence and the genetic organization of the short unique region (US) of the bovine herpesvirus type 1 (ST strain). Virology **199:**409–421.
30. **Litwin, V., W. Jackson, and C. Grose.** 1992. Receptor properties of two varicella-zoster virus glycoproteins, gpI and gpIV, homologous to herpes simplex virus gE and gI. J. Virol. **66:**3643–3651.
31. **Long, D., G. H. Cohen, M. I. Muggeridge, and R. J. Eisenberg.** 1990. Cysteine mutants of herpes simplex virus type 1 glycoprotein D exhibit temperature-sensitive properties in structure and function. J. Virol. **64:**5542–5552.
32. **Long, D., W. C. Wilcox, W. R. Abrams, G. H. Cohen, and R. J. Eisenberg.** 1992. Disulfide bond structure of glycoprotein D of herpes simplex virus types 1 and 2. J. Virol. **66:**6668–6685.
33. **Mallory, S., M. Sommer, and A. M. Arvin.** 1997. Mutational analysis of the role of glycoprotein I in varicella-zoster virus replication and its effects on glycoprotein E conformation and trafficking. J. Virol. **71:**8279–8288.
34. **McGeoch, D. J.** 1990. Evolutionary relationships of virion glycoprotein genes in the S regions of alphaherpesvirus genomes. J. Gen. Virol. **71:**2361–2367.
35. **McGinnes, L. W., and T. G. Morrison.** 1997. Disulfide bond formation is a determinant of glycosylation site usage in the hemagglutinin-neuraminidase glycoprotein of Newcastle disease virus. J. Virol. **71:**3083–3089.
36. **Mettenleiter, T. C., C. Schreurs, F. Zuckermann, and T. Ben-Porat.** 1987. Role of pseudorabies virus glycoprotein gI in virus release from infected cells. J. Virol. **61:**2764–2769.
37. **Mijnes, J. D. F., B. C. H. Lutters, A. C. Vlot, E. van Anken, M. C. Horzinek, P. J. M. Rottier, and R. J. de Groot.** 1997. Structure-function analysis of the gE-gI complex of feline herpesvirus: mapping of gI domains required for gE-gI interaction, intracellular transport, and cell-to-cell spread. J. Virol. **71:** 8397–8404.
38. **Mijnes, J. D. F., L. M. van der Horst, E. van Anken, M. C. Horzinek, P. J. M. Rottier, and R. J. de Groot.** 1996. Biosynthesis of glycoproteins E and I of feline herpesvirus: gE-gI interaction is required for intracellular transport. J. Virol. **70:**5466–5475.
39. **Mijnes, J. D. F., and R. J. de Groot.** Unpublished observations.
40. **Mulder, W. A., L. Jacobs, J. Priem, G. L. Kok, F. Wagenaar, T. G. Kimman, and J. M. Pol.** 1994. Glycoprotein gE-negative pseudorabies virus has a reduced capability to infect second- and third-order neurons of the olfactory and trigeminal routes in the porcine central nervous system. J. Gen. Virol. **75:**3095–3106.
41. **Neidhardt, H., C. H. Schröder, and H. C. Kaerner.** 1987. Herpes simplex virus type 1 glycoprotein E is not indispensable for viral infectivity. J. Virol. **61:**600–603.
42. **Olson, J. K., and C. Grose.** 1998. Complex formation facilitates endocytosis of the varicella-zoster virus gE:gI Fc receptor. J. Virol. **72:**1542–1551.
43. **Petrovskis, E. A., J. G. Timmins, T. M. Gierman, and L. E. Post.** 1986. Deletions in vaccine strains of pseudorabies virus and their effect on synthesis of glycoprotein gp63. J. Virol. **60:**1166–1169.
44. **Rajcani, J., U. Herget, and H. C. Kaerner.** 1990. Spread of herpes simplex virus (HSV) strains SC16, ANG, ANGpath and its glyC minus and glyE minus mutants in DBA-2 mice. Acta Virol. **34:**305–320.
45. **Saiki, R. K., D. H. Gelfand, S. Stoffel, S. J. Scharf, R. Higuchi, G. T. Horn, K. B. Mullis, and H. A. Erlich.** 1988. Primer-directed enzymatic amplification of DNA with a thermostable DNA polymerase. Science **239:**487–491.
46. **Sambrook, J., E. F. Fritsch, and T. Maniatis.** 1989. Molecular cloning: a laboratory manual, 2nd ed. Cold Spring Harbor Laboratory, Cold Spring Harbor, N.Y.
47. **Schägger, H., and G. von Jagow.** 1987. Tricine-sodium dodecyl sulfate-polyacrylamide gel electrophoresis for the separation of proteins in the range from 1 to 100 kDa. Anal. Biochem. **166:**368–379.
48. **Sussman, M. D., R. K. Maes, J. M. Kruger, S. J. Spätz, and P. J. Venta.** 1995. A feline herpesvirus-1 recombinant with a deletion in the genes for glycoproteins gI and gE is effective as a vaccine for feline rhinotracheitis. Virology **214:**12–20.
49. **Tirabassi, R. S., R. A. Townley, M. G. Eldridge, and L. W. Enquist.** 1997. Characterization of pseudorabies virus mutants expressing carboxy-terminal truncations of gE: evidence for envelope incorporation, virulence, and neurotropism domains. J. Virol. **71:**6455–6464.
50. **van Engelenburg, F. A. C., M. J. Kaashoek, F. A. M. Rijsewijk, L. van den Burg, A. Moerman, A. L. J. Gielkens, and J. T. van Oirschot.** 1994. A glycoprotein E deletion mutant of bovine herpesvirus 1 is avirulent in calves. J. Gen. Virol. **75:**2311–2318.
51. **van Vliet, K. E., L. A. de Graaf Miltenburg, J. Verhoef, and J. A. van Strijp.** 1992. Direct evidence for antibody bipolar bridging on herpes simplex virus-infected cells. Immunology **77:**109–115.
52. **Weeks, B. S., P. Sundaresan, T. Nagashunmugam, E. Kang, and H. M. Friedman.** 1997. The herpes simplex virus-1 glycoprotein E (gE) mediates IgG binding and cell-to-cell spread through distinct gE domains. Biochem. Biophys. Res. Commun. **235:**31–35.
53. **Whealy, M. E., J. P. Card, A. K. Robbins, J. R. Dubin, H.-J. Rziha, and L. W. Enquist.** 1993. Specific pseudorabies virus infection of the rat visual system requires both gI and gp63 glycoproteins. J. Virol. **67:**3786–3797.
54. **Whitbeck, J. C., A. C. Knapp, L. W. Enquist, W. C. Lawrence, and L. J. Bello.** 1996. Synthesis, processing, and oligomerization of bovine herpesvirus 1 gE and gI membrane proteins. J. Virol. **70:**7878–7884.
55. **Willemse, M. J., W. S. K. Chalmers, and P. J. A. Sondermeijer.** 1996. *In vivo* properties of a feline herpesvirus type 1 mutant carrying a lacZ insertion at the gI locus of the unique short segment. Vaccine **14:**1–5.
56. **Willemse, M. J., I. G. Strijdveen, S. H. van Schooneveld, M. C. van den Berg, and P. J. Sondermeijer.** 1995. Transcriptional analysis of the short segment of the feline herpesvirus type 1 genome and insertional mutagenesis of a unique reading frame. Virology **208:**704–711.
57. **Yao, Z., and C. Grose.** 1994. Unusual phosphorylation sequence in the gpIV (gI) component of the varicella-zoster virus gpI-gpIV glycoprotein complex (VZV gE-gI complex). J. Virol. **68:**4204–4211.
58. **Yao, Z., W. Jackson, B. Forghani, and C. Grose.** 1993. Varicella-zoster virus glycoprotein gpI/gpIV receptor: expression, complex formation, and antigenicity within the vaccinia virus-T7 RNA polymerase transfection system. J. Virol. **67:**305–314.
59. **Zhu, Z., Y. Hao, M. D. Gershon, R. T. Ambron, and A. A. Gershon.** 1996. Targeting of glycoprotein I (gE) of varicella-zoster virus to the *trans*-Golgi network by an AYRV sequence and an acidic amino acid-rich patch in the cytosolic domain of the molecule. J. Virol. **70:**6563–6575.
60. **Zsak, L., F. Zuckermann, N. Sugg, and T. Ben-Porat.** 1992. Glycoprotein gI of pseudorabies virus promotes cell fusion and virus spread via direct cell-to-cell transmission. J. Virol. **66:**2316–2325.
61. **Zuckermann, F. A., T. C. Mettenleiter, C. Schreurs, N. Sugg, and T. Ben-Porat.** 1988. Complex between glycoproteins gI and gp63 of pseudorabies virus: its effect on virus replication. J. Virol. **62:**4622–4626.